IEEK Transactions on Smart Processing and Computing

A Concurrent Triple-band RF Energy Harvesting Circuit for IoT Sensor Networks

Luong Duy Manh[1], Phan Thi Bich[1], Nguyen Thuy Linh[1], Nguyen Huy Hoang[1], Xuan Nam Tran[1] and Koichiro Ishibashi[2]

[1] Le Quy Don Technical University, 236 Hoang Quoc Viet, Hanoi, Vietnam duymanhcs2@mta.edu.vn
[2] The University of Electro-Communications, 1 Chome-5-1 Chofugaoka, Chofu, Tokyo 182-8585, Japan ishibashi@uec.ac.jp

Abstract— dwkim@cs.utah.edu

***** Corresponding Author: Luong Duy Manh

Received ....; Revised ....; Accepted .....; Published .....

** Extended from a Conference: Preliminary results of this paper were presented at the ICGHIT2020. This present paper has been accepted by the editorial board through the regular reviewing process that confirms the original contribution.*

***Abstract*:** In this paper, a concurrent triple-band RF energy harvesting circuit is proposed. The proposed circuit incorporates a triple-band microstrip antenna combining with a low-loss diplexer and three compact RF rectifiers. The proposed circuit operates concurrently at three popular frequency bands: GSM-900, GSM-1800, and 2.45 GHz. To improve output voltage and efficiency, three rectifiers are connected in a stacked topology. The simulated and measured results demonstrate that the circuit operates well in concurrent bands. Moreover, the proposed circuit exhibits low-complexity in structure and compactness in size. These advantages make the circuit a highly potential candidate for running low-power devices in IoT sensor networks.

***Keywords*:** RFEH, Antenna, Rectifier, Triple-band

1. Introduction

In the era of the 4th revolution, the number of smart radio devices is increasing remarkably, especially the number of wireless sensors used in wireless sensor networks, smart devices in IoT networks or body-mounted, wearable radio devices, wireless sensors for monitoring drought, natural disasters, traffic sensors, etc. They are all low-power radio devices that consume small power and are deployed with high density in the networks. One of the most critical requirements for these smart devices is the ability to remain un-interrupted operation over long periods. This is because these radio devices are deployed in complex locations such as inside the human body, in remote and inaccessible areas, such as in riverbeds, in complex terrains such as offshore seas and islands, or in the mountains where accessing to electrical power sources or the replacement of DC power sources such as batteries is impossible and complicated. Besides, the DC battery has a certain lifespan and the replacement cannot be done immediately or facing stringent challenges when the devices are deployed in hard-to-reach and remote locations or inside the human body. In terms of the environment, the battery is a chemical source that is harmful to the environment. Hence, finding new sources of renewable energy or alternative green energy sources helps to protect the environment. These reasons have led to the emergence of research on renewable energy sources for running these sensor devices without the need for a battery. Recently, there are energy harvesting techniques from various available sources in the environment including thermal energy [1, 2], solar energy [3, 4], and mechanical energy [5]. However, these energy sources depend largely on the weather condition and they are not continuous sources. Although solar energy has high levels, it is only available when sunlight is available. Wind power is difficult to implement for body-mounted radio devices and wind power is not continuous and stable. Heat energy and oscillation are small and discontinuous. The biggest drawback of these renewable energy sources is the discontinuity of the energy source. In addition to these energy sources, radio frequency (RF) energy is recently a very promising renewable energy source due to the increasing number of wireless signal sources in the environment including mobile base station [6], Wi-Fi [7], radio and television transmitters [8-10], Bluetooth, laptop, and mobile phones [11-14]. The RF energy sources are not only continuous but highly condensed in the environment. These superior advantages make this type of energy source to be very promising for utilizing in many realistic applications.

However, one of the major downsides of the RF energy source is relatively low power density which is about 1 μW/cm^2. Hence, the RF energy harvesting systems need to operate efficiently to supply sufficient energy to smart devices or sensors in the network. Nevertheless, the existing RF energy harvesting systems are now facing inherent drawbacks so that efficient extraction of energy from the RF sources cannot be fulfilled. These main drawbacks can be listed in the following aspects: antenna with low impedance, low gain, low efficiency, and narrow bandwidth; active devices with low-efficiency rectifying operation resulting in low output voltage; impedance matching circuits with narrowband operation and less efficient at multiband operation; total size of the system is bulky and not appropriate for practical applications. Various solutions have been introduced and many research works have been reported to surmount these drawbacks for years. In terms of multiband operation, in [15] authors proposed a dual-band antenna for RF energy harvesting (RFEH) systems. The antenna operated concurrently in Wi-Fi bands: 2.45 GHz and 5 GHz. The antenna was fabricated on a RT/Duroid 5870 substrate. The radiation pattern was quasi-omnidirectional. The size of this antenna, however, was relatively large. Moreover, the output voltage was just on the order of 1 V with very high input power from 0 dBm to 15 dBm. This high input power is not suitable for harvesting ambient RF energy as the RF power in the environment is usually very low, basically below 0 dBm. Also, in [16] authors presented their RFEH system to operate in three bands LTE 700 MHz, GSM 850 MHz, and ISM 900 MHz with using just a single circuit. The system was tested in Boston city, US. This work employed a zero-bias Schottky diode HSMS-285C as the active device and efficiency could achieve as high as 45% with a low input power range from -25 dBm to -5 dBm. However, the system was very bulky, especially in the antenna part, thus it is not appropriate for integrated applications and commercialization. S. Shen, et al. [17] reported a triple-band rectifier operating at GSM-900, GSM-1800, and UMTS-2100 bands. This circuit could achieve high efficiency of 40% at a power density of greater than 500 μW/m^2. Although this circuit could offer relatively high efficiency at triple-band operation, its delivered output voltage was relatively small, 0.6 V. S. Chandravanshi, et al. in [18] proposed a triple band differential rectenna for RF energy harvesting applications. It operated at UMTL, lower WLAN/Wi-Fi, and WiMAX bands. This circuit achieved a maximum efficiency of 53% at 2 GHz, 31% at 2.5 GHz, and 15.56% at 3.5 GHz. However, the circuit was not in the integrated circuit, and the gain of the antenna was low. In terms of efficiency enhancement of the rectifier, authors in [19] proposed a high-efficiency rectifier used with a fractal loop antenna. The rectifier could deliver an efficiency of 61%. The output DC voltage was 1.8 V with a 12 kΩ resistor for 10 μW/cm^2 power density at 1.8 GHz. This was considered a compact and high-efficiency rectifier. Nevertheless, the output voltage was still low and this rectifier just worked in a single-band. Authors in [20] presented a RF energy harvester designing to maximize the harvested RF energy in the 902 MHz to 928 MHz bands. This harvester exhibited an efficiency of 32% at -15 dBm input power and an output DC voltage of 3.2 V to a 1 MΩ load. This circuit offered relatively high efficiency and output voltage but not in an integrated form and moreover, it only operated in a narrow band.

In this paper, we develop a novel compact and low-cost RFEH circuit operating concurrently at three frequency bands: GSM-920, GSM-1800, and 2.45 GHz. These are three most popular available frequency bands with high power density in the environment. If using a dual-band circuit, it may not have sufficient energy for powering the IoT sensors. Moreover, using a quadruple-band or higher-order circuits increase the complexity thus increasing circuit size as well as losses in the PCB. The circuit includes a compact triple-band antenna combining with a low-loss diplexer, and three rectifiers operating at each frequency band as shown in Fig. 1. As indicated in the figure, the circuit incorporates a triple-band antenna, a low-loss diplexer and three rectifiers connecting to each other using a stacked topology. This topology is employed to boost the output voltage efficiently because the output voltage of the lower stage becomes the reference voltage of the next higher stages. The antenna was fabricated on a low-cost FR4 substrate for compact size and reduction of fabrication cost. In addition, the antenna was designed to operate simultaneously at three popular frequency bands which are GSM-920, GSM-1800, and 2.45 GHz for WiFi. The simulated and measured results demonstrate that the proposed RFEH circuit can obtain high efficiency at low input power and high output voltage while still ensure the compactness of the entire circuit.

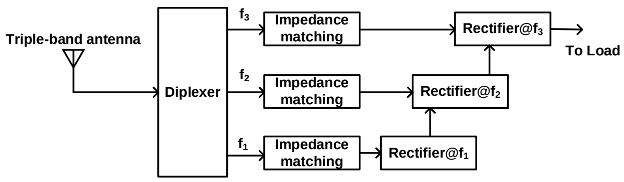

Figure 1. Schematic diagram of the proposed RFEH circuit.

The rest of the paper is organized as follows: Section 2 presents the design procedure and simulated results of each part of the RFEH circuit, then experimental validation is presented in Section 3, and finally, Section 4 concludes the paper.

2. Circuit design

In this section, the design of each part in the proposed circuit is presented. As shown in Fig. 1, the RFEH circuit consists of three main parts, that are antenna, diplexer, and rectifiers. Firstly, the design of the triple-band antenna is described in the next subsection.

2.1. Antenna design

The antenna is designed and fabricated using microstrip technology on the FR4 substrate for integration capability and low-cost. The antenna aims at operating concurrently at three bands: GSM-900, GSM-1800, and 2.45 GHz. In addition to the multi-band operation target, the antenna is designed to have an omnidirectional feature while still ensure sufficient gain. The purpose of omni-direction is because in realistic applications, the electromagnetic signal can come from any directions in the environment.

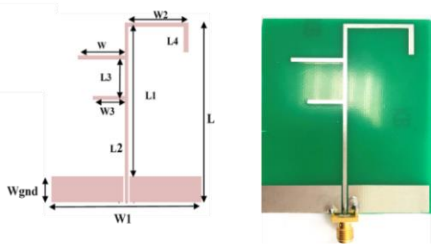

Figure 2. Triple-band antenna: Layout in ADS (left) and fabricated prototype (right).

Figure 2 shows the layout and fabricated prototype of the triple-band microstrip antenna. Here, the antenna is designed in the form of a microstrip dipole having reflective metal planes in the same layer with the dipole. The antenna includes three stubs with different lengths which are used to tune the resonant frequency of the antenna at each operation frequency band. The first stub with length of W3 is tuned at GSM-900 band while the second one with a length of W is tuned at the GSM-1800 band and the last one with a length of W2 + L is tuned at 2.45 GHz band. It is noted that the last stub is bent intentionally to save the circuit space. The width of the main microstrip line is chosen to be 0.5 mm which is equivalent to 50 Ω line. Dimensions of the antenna are given in Table 1.

Table 1. Antenna dimensions

Dimension	Value (mm)	Dimension	Value (mm)
L	90	Wgnd	10
L1	78.5	W	1.5
L2	30	W1	62.4
L3	14.3	S	0.5
L4	10	W2	26.5
W3	13.25	W4	19.5

To evaluate the antenna performance for using in the RFEH circuit, it is first checked radiation pattern along with gain. This is done in ADS2016 simulator with using an electromagnetic (EM) analysis.

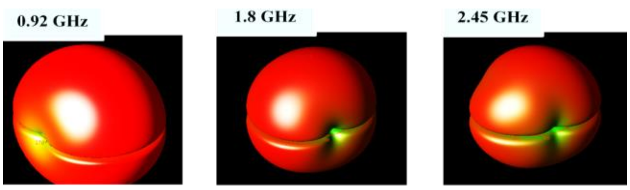

Figure 3. Simulated radiation pattern of the triple-band antenna.

In Figure 3 which shows the radiation pattern of the designed antenna at each operation frequency, it is seen that the radiation pattern is almost omnidirectional at all the operation frequencies. The simulated gain of the antenna at each frequency is given as follows: 1.54 dBi@920 MHz; 2.08 dBi@1.8 GHz; 3.02 dBi@2.45 GHz. These simulated results validate the appropriateness of the design. Here, the antenna was fabricated on the FR4 substrate with following parameters: dielectric constant = 4.5; dissipation factor = 0.014; thickness = 0.8 mm; copper thickness = 35 μm. Figure 4 describes teh experimental setup to evaluate the return loss of the fabricated antenna.

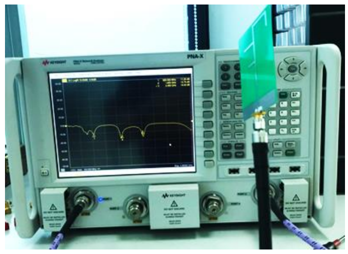

Figure 4. Experimental setup for return loss measurement of the antenna.

A vector signal analyzer (VNA) from Keysight (N5242A) is employed to measured return loss (S_{11}) of the antenna to check its operation frequencies.

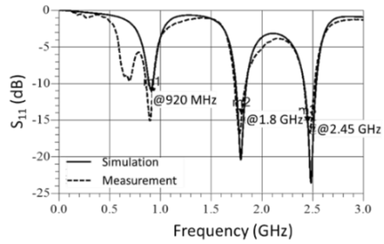

Figure 5. Simulated and measured results of the triple-band antenna.

The simulated and measured results of S_{11} shown in Fig. 5 implies that the antenna resonates at three frequencies: 920 MHz, 1.8 GHz, and 2.45 GHz satisfying the requirement for multi-band operation. Moreover, it can also clearly be observed a good agreement between simulation and measurement in the figure. This validates the accuracy of the design. There is some discrepancy between simulation and measurement at a lower frequency range below 920 MHz due to some errors come from the calibration procedure. To further validate the antenna design, it is tested in a real experiment as shown in Fig. 6.

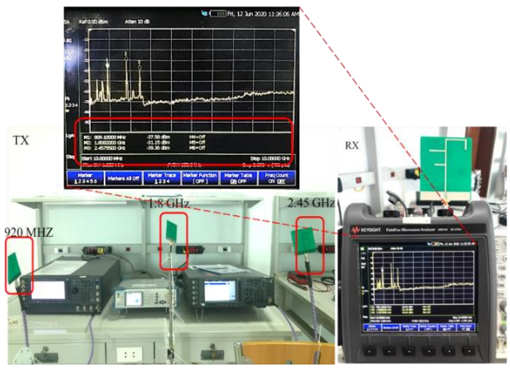

Figure 6. Realistic experiment for testing antenna.

In the realistic experiment, three signal generators connecting to three antennas are employed to transmit three signals at three operation frequencies: 920 MHz, 1.8 GHz, and 2.45 GHz. On the receiving side, the triple-band antenna is connected to a portable spectrum analyzer from Keysight. As can be seen in the figure, the antenna can receive well all the transmitted signals at three operation frequency bands indicated by the received spectrum on the spectrum analyzer. This has further validated the accuracy of the design.

2.2. Diplexer design

The diplexer is designed to split the received signal to each signal at each operation frequency then fed to each rectifier circuit. Therefore, it has to exhibit low-loss and compactness. To have the compactness, the diplexer is designed using lumped components. Figure 7 shows a co-simulation model for the diplexer which is implemented in the ADS simulator. The model includes an EM model for microstrip lines functioning as interconnects along with capacitors and inductors at three branches. Each branch consists of two parallel LC tanks combining with a lumped element which is either an inductor or capacitor.

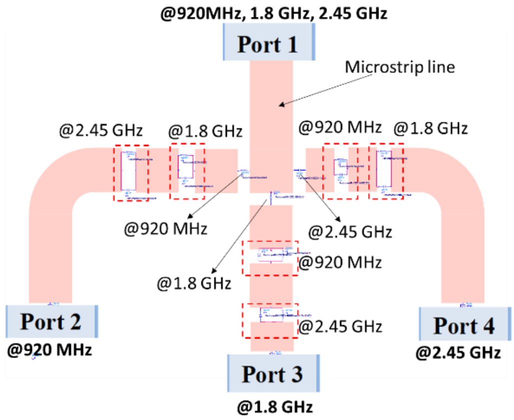

Figure 7. Co-simulation model for the designed diplexer.

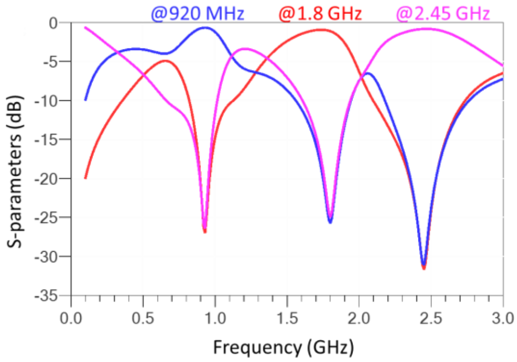

Figure 8. Simulated S-parameters of the diplexer.

Two LC tanks in each branch resonate at two resonant frequencies and the other lumped element is tuned to pass the signal having a frequency of interest. Thanks to such a technique, the diplexer is able to pass the signal at each operation frequency to each branch. The total size of this circuit is just 1.8 cm × 2 cm. The simulated performance of the diplexer is indicated in Fig. 8. It can be observed that the diplexer operates well at 920 MHz, 1.8 GHz, and 2.45 GHz. The insertion loss of each band is given as follows: -0.67 dB@920 MHz, -1.1 dB@1.8 GHz, -0.82 dB@2.45 GHz. In addition, the figure also indicates that at each frequency band of interest, the signal at the other two bands is rejected significantly indicating a high isolation characteristic.

2.3. Rectifier design

The next step is to design one of the most critical parts of the proposed RFEH circuit, the rectifier. In this study, the rectifier incorporates a matching network and a two-stage voltage doubler circuit where each stage uses two zero-bias SBD diodes (SMS7630). Here, the matching network is designed at each operation frequency band and at the same input power of -10 dBm to guarantee that the circuit can be used to collect RF energy in the environment. The diode SMS7630 is chosen because of its low-cost and relatively low threshold voltage as indicated in Fig. 9 which shows the I-V curve of this diode.

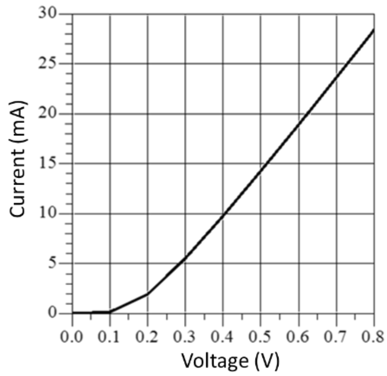

Figure 9. I-V characteristic of the SMS7630 diode.

It can be seen in the figure that, the threshold voltage of the SMS7630 is about 0.1 V. This implies that this diode is highly suitable for RFEH applications. The schematic of the single rectifier operating at a single band which is implemented in the ADS simulator is shown in Fig. 10. The rectifier is implemented in the same FR4 substrate as the antenna and the diplexer so that all the parts of the RFEH circuit can be integrated on the same substrate. As mentioned previously, the output voltage of the 920 MHz rectifier becomes the reference voltage for the 1.8 GHz rectifier, then the output voltage of the 1.8 GHz rectifier becomes a reference voltage for the 2.45 GHz. The rectifier at 920 MHz is chosen as the first stage since the power level of this band is normally highest among the three bands and this prevents the circuit from being floating at the first stage. The entire RFEH circuit which is realized by incorporating all the constituent parts is described in Fig. 11. Here, it is noted that the matching network in the 2.45 GHz rectifier branch uses an open stub for the purpose of impedance matching instead of using lumped elements.

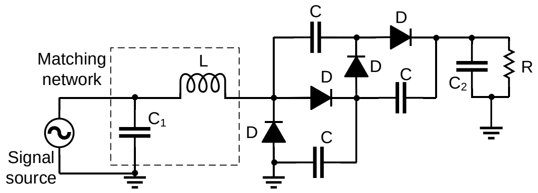

Figure 10. Schematic of a single proposed rectifier.

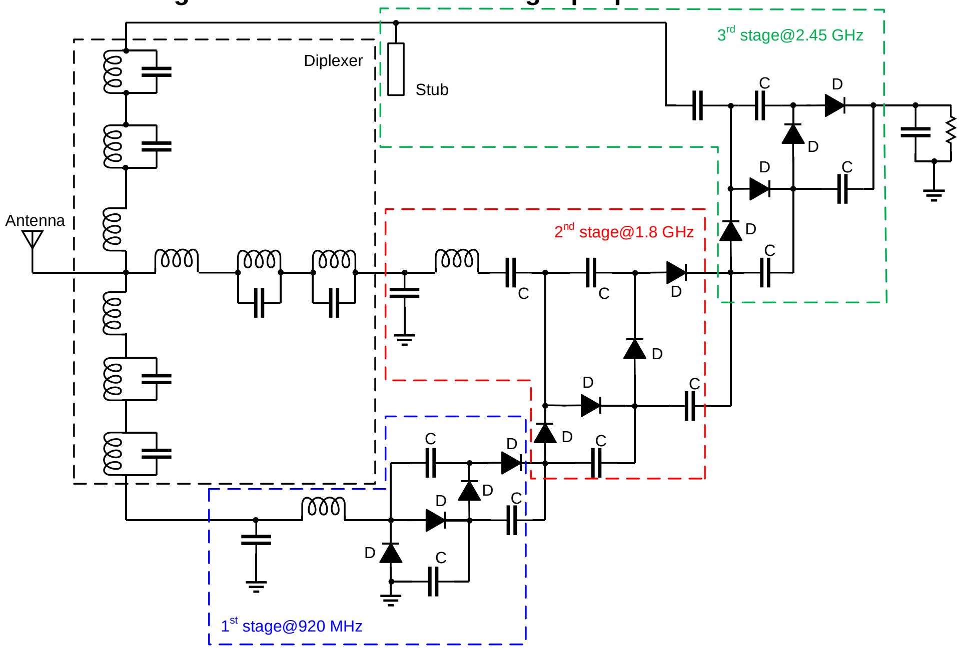

Figure 11. Schematic of the entire RFEH circuit.

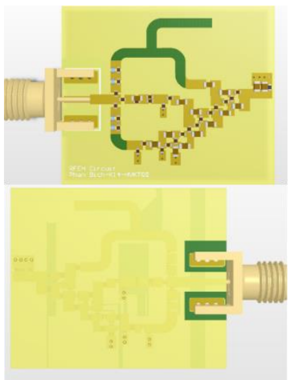

Figure 12. Layout of the final RFEH circuit: top layer (upper) and bottom layer (lower).

The layout of the final circuit for the schematic shown in Fig. 11 which is implemented in the Altium simulator is given in Fig. 12. The total circuit size of the RFEH circuit is just 2 cm × 2 cm. Figure 13 shows the simulated return loss of the rectifier in the ADS simulator to validate impedance matching at each operation frequency band. The simulated results indicate that the rectifier exhibits reasonable return loss below -10 dB at each frequency band of interest. This clearly validates the design.

Thanks to the use of the stacked structure for the voltage doubler at each frequency band in each rectifier, output DC voltage can be significantly improved as indicated in Fig. 14.

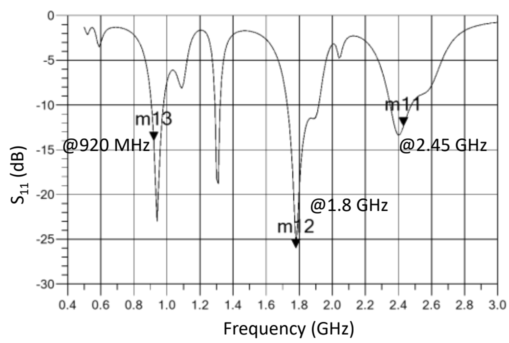

Figure 13. Simulated return loss of the rectifier.

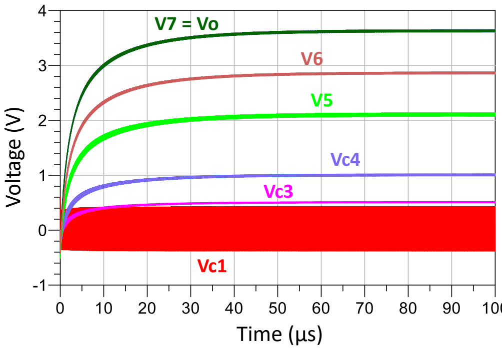

Figure 14. Simulated voltage at each node of circuit.

The figure represents the simulated voltage at each node as shown in the schematic in Fig. 11. It can be observed that Vc1 is an AC voltage while the voltages at other nodes such as Vc3, Vc4, V5, V6, and V7 are rectified voltage, thus they are DC voltages. The DC voltage of the upper stage has a higher value compared to the lower stage as explained previously. The final output DC voltage (V7 or Vo) can be relatively (more than 3.5 V) at the input level of -10 dBm. Additionally, the RF-DC efficiency of the proposed RFEH circuit is given in Fig. 15.

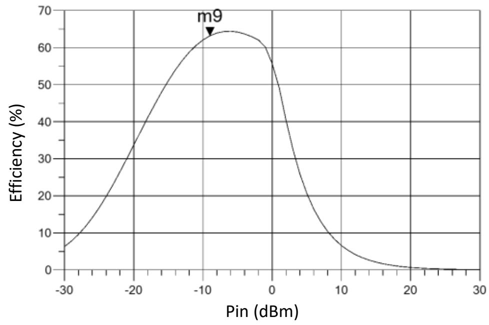

Figure 15. Simulated RF-DC efficiency of the rectifier.

It can be seen that, the rectifier can achieve a high efficiency due to the high output voltage. More than 60% of efficiency at -10 dBm input is clearly seen in the figure. Here, value of the load resistor is 200 kΩ.

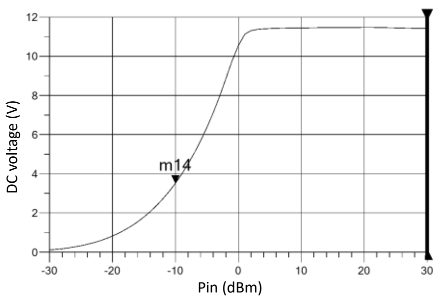

Figure 16. Simulated output voltage with input power.

The output voltage can be increased much more if the collected input power is higher than -10 dBm as demonstrated in Fig. 16 above. It can be clearly seen that the DC voltage can be obtainable from 3.8 V to 10.5 V when input power varies from -10 dBm to 0 dBm.

3. Experiment

The fabricated RFEH circuit PCB is given in Fig. 17. The circuit was fabricated on a low-cost and moderate performance FR4 substrate. The total size is very compact which is 2 cm × 2 cm.

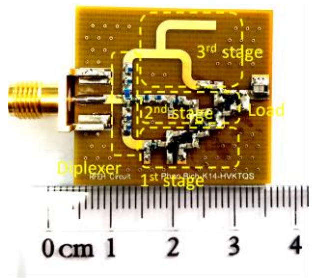

Figure 17. Fabricated prototype of the RFEH circuit.

To test performance of the circuit, its return loss is first checked without connecting with the antenna.

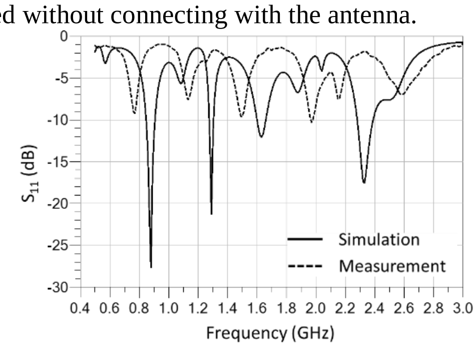

Figure 18. Measured return loss of the RFEH circuit.

Figure 18 above shows the measured return loss of the rectifier circuit without an antenna. The designed circuit exhibits relatively low return loss at three bands of interest that are GSM-900, GSM-1800 bands, and 2.45 GHz band. It is noted that the measured S_{11} is slightly shifted over the simulated one due to tolerance in the fabrication process of the microstrip PCB.

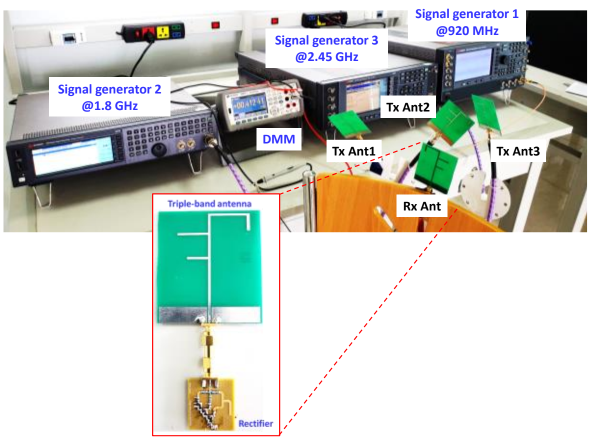

Figure 19. Experimental setup for output DC voltage measurement.

Figure 19 shows the experimental setup for the measurement of output DC voltage of the designed RFEH circuit connecting with the triple-band antenna. Here, three

Keysight RF signal generators (SG) are connected to three triple-band transmitting antennas (Tx Ant1, Tx Ant2, and Tx Ant3) to generate RF signal at three bands of interest. The receiving circuit is the proposed rectifier connecting with the triple-band receiving antenna (Rx Ant) through a male SMA-male SMA adapter. The output DC voltage is measured using a digital multimeter (DMM) from Keysight. All the four antennas point towards each other to increase the receiving signal strength. RF power of each SG was 10 dBm and measured power at the received antenna was -22 dBm. The distance between Tx and Rx was 20 cm. The received RF power was measured directly from the Rx antenna connecting to a spectrum analyzer. This low received power was caused by various loss factors including antenna polarization mismatch, connector loss, return loss of antenna. The efficiency was calculated to be 12% at the received power of -22 dBm on a 200 kΩ load.

Figure 20. Measured output DC voltage according to different states of RF signal generators.

The measured results are indicated in Fig. 20 for various states of the SGs. It can be seen that when turning on each SG alternately at the corresponding frequency band, the output DC voltage is very low, that is 0.2 V@920 MHz, 0.04 V@1.8 GHz, 0.08 V@2.45 GHz. However, when turning on all the SGs simultaneously, the output DC voltage increases significantly. This value is about 0.64 V. This implies that the designed circuit operates well at three frequency bands concurrently. Nevertheless, the output DC voltage is still small compared with the simulation. This should be caused by the in-accuracies of the diode model in the ADS and PCB fabrication process.

Figure 21 and Fig. 22 show the measured output voltage waveform of the circuit prototype.

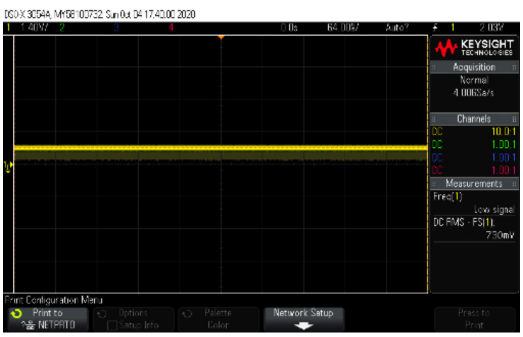

Figure 21. Measured output voltage waveform.

Figure 22. Detailed information of the measured output voltage waveform shown in Fig. 21.

Figure 21 shows the voltage waveform on a Keysight digital oscilloscope DSOX3054A and Fig. 22 indicates the detailed information of this waveform. It can be observed that the frequency of the waveform is low-frequency indicating the rectifying behavior and the DC RMS value is 700 mV which is the measured output rectified voltage.

Table 1 compares the performance of the present study with other recent works.

Table 1. Performance comparison

Related work	*RF source*	*RF Power Sensitivity*	*Output voltage*	*Size*	*Range/ Antenna gain*	*Technology*
This work	GSM900; GSM180; WiFi	-22 dBm	0.64 V	8 cm x 11 cm (W x L)	20 cm/(1.5 dBi; 2 dBi; 3 dBi)	SMS-7630
A. Bakkali [21]	WiFi (2.45 GHz, 5 GHz)	10 dBm	1.3 V	NA	60 cm/4 dBi	SMS-7630-079LF
K. Dey [22]	GSM900; GSM1800	NA	0.04 V – 0.09 V	NA	NA	HSMS-2850
P. Kim [23]	881 MHz; 2.4 GHz	22 dBm	6.8 V – 7.0 V	3 cm x 2.5 cm (w/o antenna)	From SG	HSMS-2822
P. Rengalakshmi [24]	GSM900	-10 dBm	0.6 V	NA	From SG (simulation)	HSMS285X

It can be seen that proposed circuit delivers moderate voltage when collecting RF energy sources from ambient environment with relatively low RF power of -22 dBm while still ensuring the compact size of the entire circuit. However, the distance between the Tx and Rx is still short due to the low gains of the designed antenna.

5. Conclusion

In this paper, a novel concurrent triple-band RFEH circuit is proposed for potentially running low-power sensors in IoT sensor networks. The proposed circuit operates concurrently at three popular frequency bands: GSM-900, GSM-1800, and 2.45 GHz. All parts in the circuit are implemented on the same low-cost FR4 substrate for integration capability. The output DC voltage and efficiency of the circuit are improved by using the stacked structure for the three rectifiers. Simulation and measurement have validated the proposed design methodology and performance of the RFEH circuit. The measured output DC voltage of the circuit is on the level of 643 mV when collecting RF signals simultaneously from three SGs at 920 MHz, 1.8 GHz, and 2.45 GHz. The final circuit size of the triple-band antenna and rectifier circuit is 9 cm × 6.2 cm and 2 cm × 2 cm, respectively. Therefore, the proposed circuit can become a promising candidate for running low-power sensors in IoT sensor networks.

Acknowledgement

This research was supported by the ASEAN IVO 2020 project entitled “An Energy Efficient, Self-Sustainable, and Long Range IoT System for Drought Monitoring and Early Warning”.

References

[1] L. Mateu, et al., “Energy harvesting for wireless communication systems using thermo-generators,” in *Proc. of the 21st Conference on Design of Circuits and Integrated Systems (DCIS ’06)*, Barcelona, Spain, Nov. 2006.

[2] H. Bottner, et al., “New thermoelectric components using microsystem technologies,” *Journal of Micro-electromechanical Systems*, Vol. 13, No. 3, pp. 414–420, 2004.

[3] C. Wang, et al., “Combining Solar Energy Harvesting with Wireless Charging for Hybrid Wireless Sensor Networks”, *IEEE Transactions on Mobile Computing*, Vol. 17, No. 3, Mar. 2018.

[4] B. Mulla, et al., “Multiband Metamaterial Absorber Design Based on Plasmonic Resonances for Solar Energy Harvesting”, *Plasmonics*, No. 11, pp. 1313–1321, 2016.

[5] S. Kim, et al., “Electrochemically driven mechanical energy harvesting”, *Nat Commun*, No. 7, 2016.

[6] S. Kitazawa, et al., “Energy harvesting from ambient RF sources,” *in IEEE MTT-S Int. Microw. Symp. Workshop*, 2012, pp. 39–42.

[7] Y. Shi, et al., "Design of a Novel Compact and Efficient Rectenna for WiFi Energy Harvesting," *Progress In Electromagnetics Research C*, Vol. 83, pp. 57-70, 2018.

[8] T. Sogorb, et al., “Studying the feasibility of energy harvesting from broadcast RF station for WSN,” *in Proc. of the IEEE Instrumentation and Measurement Technology Conference Proceedings (IMTC ’08)*, pp. 1360–1363, IEEE, Victoria, Canada, May 2008.

[9] T. S. Salter, “Low power smart-dust receiver with novel applications and improvements of an RF power harvesting circuit”, *[Ph.D. thesis]*, University of Maryland, 2009.

[10] C. Mikeka, et al., “Sustainable energy harvesting technologies—past, present and future,” in Design Issues in Radio Frequency Energy Harvesting System, Ed., InTech, Vienna, Austria, 2011.

[11] T. B. Lim, et al., “Feasibility study on ambient RF energy harvesting for wireless sensor network,” *in Proc. of the IEEE MTT-S International Microwave Workshop Series on RF and Wireless Technologies for Biomedical and Healthcare Applications (IMWS-BIO ’13)*, pp. 1–3, IEEE, Singapore, Dec. 2013.

[12] S. N. Deepa, et al., “RF energy harvesting using 900MHz of mobile signal frequency to charging the mobile battery”, *2017 International Conference on Innovations in Green Energy and Healthcare Technologies (IGEHT)*, Coimbatore, India, pp. 16-18, Mar. 2017.

[13] M. Arrawatia, et al., "Broadband rectenna array for RF energy harvesting," *2016 IEEE International Symposium on Antennas and Propagation (APSURSI)*, pp. 1869-1870, 2016.

[14] M. J. M. Silva, et al., "Radio frequency energy harvesting using series resonant circuit," *2017 IEEE 18th Wireless and Microwave Technology Conference (WAMICON)*, Cocoa Beach, FL, pp. 1-4, 2017.

[15] A. Bakkali, et al., “A Dual-Band Antenna for RF Energy Harvesting Systems in Wireless Sensor Networks”, *Journal of Sensors*, Vol. 2016, 2016.

[16] U. Muncuk, et al., "Multiband Ambient RF Energy Harvesting Circuit Design for Enabling Battery-less Sensors and IoT," *IEEE Internet of Things Journal*, Vol. 5, No. 4, pp. 2700-2714, Aug. 2018.

[17] S. Shen, et al., "A Dual-Port Triple-Band L-Probe Microstrip Patch Rectenna for Ambient RF Energy Harvesting," *IEEE Antennas and Wireless Propagation Letters*, Vol. 16, pp. 3071-3074, 2017.

[18] S. Chandravanshi, et al., "Design of Dual Band Compact Wireless Energy Harvesting Circuit for GSM and WLAN Band," *2018 IEEE MTT-S International Microwave and RF Conference (IMaRC)*, Kolkata, India, pp. 1-4, 2018.

[19] M. Zeng, et al., "A Compact Fractal Loop Rectenna for RF Energy Harvesting," *IEEE Antennas and Wireless Propagation Letters*, Vol. 16, pp. 2424-2427, 2017.

[20] Z. Hameed, et al., “Design of impedance matching circuits for RF energy harvesting systems”, *Microelectronics Journal*, Vol. 62, pp. 49-56, Apr. 2017.

[21] A. Bakkali, et al. "A Dual-Band Antenna for RF Energy Harvesting Systems in Wireless Sensor Networks," *Journal of Sensors*, Vol. 2016, Article ID 5725836, 8 pages, 2016.

[22] K. Dey, et al. " Design of dual band rectifiers for energy harvesting applications," Journal of Sensors, 2018 *International Applied Computational Electromagnetics Society Symposium (ACES)*, Denver, CO, USA, 2018.

[23] P. Kim, et al. "A dual-band RF energy harvesting using frequency limited dual-band impedance matching," *Progress In Electromagnetics Research*, Vol. 141, pp. 443-461, 2013.

[24] P. Rengalakshmi, et al. "Rectifier for RF Energy Harvesting," *International Journal of Computer Applications*, Vol. 143, No. 10, 2016.

Luong Duy Manh received the B.S. and M.S. degrees in Physics from Hanoi University of Science (HUS), a member of Vietnam National University (VNU), Hanoi, Vietnam, in 2005 and 2007, respectively, and the D.E. degree in Electronics Engineering from the University of Electro-Communications (UEC), Tokyo, Japan, in March 2016. He worked at Graduate School of Engineering Science, Osaka

University, Japan as a postdoctoral researcher from April 2016 to June 2017. He is currently a lecturer at Le Quy Don Technical University, Hanoi, Vietnam. His research interests include development of microwave semiconductor devices and circuits and terahertz (THz) integrated systems for wireless communication applications based on resonant tunneling diodes (RTDs) and photonic crystals.

Phan Thi Bich received M.E degree from Le Quy Don Technical University, Hanoi, Vietnam in 2020 in Electronics Engineering. She is now working at Ace Antenna Co., Ltd. Her research interests include design of waveguide filter and semiconductor circuits.

Nguyen Thuy Linh received the B.E. and M.E. degrees in Electronics Engineering from Le Quy Don Technical University, Hanoi, Vietnam, in 2009 and 2013, respectively, and the D.E. degree in Electronics Engineering from the University of Electro-Communications (UEC), Tokyo, Japan, in March 2020. She is currently a lecturer at Le Quy Don Technical University, Hanoi, Vietnam. Her research interests include development of RF energy harvesting system using CMOS technology.

Nguyen Huy Hoang received the B.E., M.E. and D.E. degrees in Electronics Engineering from Le Quy Don Technical University, Hanoi, Vietnam, in 1996, 1999 and 2006, respectively. He is currently head of Radio Engineering Fundamental department at Le Quy Don Technical University, Hanoi, Vietnam. His research interests include design of RF and microwave circuits.

Xuan Nam Tran (Member, IEEE) received the master of engineering degree in telecommunications engineering from the University of Technology Sydney, Ultimo, NSW, Australia, in 1998, and the doctor of engineering degree in electronic engineering from The University of Electro-Communications, Chofu, Japan, in 2003. He is currently a Full Professor and the Head of a strong research group on advanced wireless communications with Le Quy Don Technical University, Hanoi, Vietnam. From November 2003 to March 2006, he was a Research Associate with the Information and Communication Systems Group, Department of Information and Communication Engineering, The University of Electro-Communications. Since 2006, he has been with Le Quy Don Technical University. His research interests are in the areas of space-time signal processing for communications such as adaptive antennas, space-time coding, MIMO, spatial modulation and cooperative communications. He was the recipient of the 2003 IEEE AP-S Japan Chapter Young Engineer Award, and the corecipient of two best papers from The 2012 International Conference on Advanced Technologies for Communications and The 2014 National Conference on Electronics, Communications and Information Technology. He is the founding Chair and currently the Chapter Chair of the Vietnam Chapter of IEEE Communications Society. He is a member of IEICE and the Radio-Electronics Association of Vietnam (REV).

Koichiro Ishibashi received PhD degree from Tokyo Institute of Technology, Tokyo, Japan in 1985 in Applied Electronics. After that, he joined Central Research Laboratory, Hitachi Ltd in 1985, where he investigated low power technologies for SH microprocessors and high-density SRAMs. He worked for Renesas Electronics from 2004 to 2011, where he developed low power IPs, mainly for SOCs used in mobile phones. He has been a Professor at The University of Electro-Communications, Tokyo, Japan since 2011. He has presented more than 150 papers at international conferences and have published papers in numerous journals. He was awarded R&D 100 for the development of SH4 Series Microprocessor in 1999. He is a Member of IEICE and a Fellow of IEEE. His current research interests include IoT technologies including ultra-low power LSI design technology, technologies for energy harvesting sensor networks and applications and bio sensor technology.